Sequential Time-Frequency Signature Estimation of Multi-Component FM Signals

Vaishali S. Amin [†], Yimin D. Zhang [†], and Braham Himed [‡]

[†] Department of Electrical and Computer Engineering, Temple University, Philadelphia, PA, 19122, USA
[‡] RF Technology Branch, Air Force Research Laboratory, AFRL/RYMD, Dayton, OH, 45433, USA

***Abstract*—In this paper, we consider a challenging problem of accurate instantaneous frequency (IF) estimation of multi-component non-linear frequency modulated (FM) signals, which may have distinct amplitude levels, in the presence of burst missing data samples. We propose a technique, in which the signal components are sequentially estimated from the strongest component to the weaker ones. First, the time-frequency (TF) representation of the received signal is obtained after applying a signal-adaptive TF kernel. Then, the IF of the strongest signal component is estimated to reconstruct its waveform, and its contribution is removed from the signal through orthogonal projection. The procedure is successively implemented for weaker signal components until the residual becomes negligible. The refined estimation of the signal components is independent of the missing data positions. The proposed technique successfully resolves signal components with distinct amplitude levels and achieves concentrated TF representations by mitigating the undesired effects of cross-terms and artifacts due to the burst missing data samples. Simulation results confirm the effectiveness of the proposed approach.**

***Index Terms*—Burst missing samples, FM signals, sequential estimation, time-frequency representation, compressive sensing.**

I. Introduction

Non-stationary frequency modulated (FM) signals are commonly observed in the fields of radar, sonar, radio astronomy, biomedical applications, wireless communications, and audio/video processing [1]. Time-frequency (TF) analyses have been widely used as a powerful means to accurately represent, analyze, and process such FM signals [2], [3]. In practice, noise removal, line-of-sight obstruction, and multipath fading may cause missing data in the received signals. The scenarios of burst missing samples exist as a result of impulsive noise, outlier removal, interference suppression, and obstruction or fading that lasts for multiple sampling intervals. Burst missing samples cause sinc-like artifact patterns around the true instantaneous frequencies (IFs) in the TF domain, thus obstructing the detection of true TF signatures of the sources or targets [4]. On the other hand, in radar target detection and tracking, target returns are often modeled as multi-component non-linear FM signals, and their magnitude may significantly differ due to, e.g., different target ranges. Weaker signals are more vulnerable to artifacts and noise and thus are more difficult to be detected.

The work of V. S. Amin and Y. D. Zhang is supported in part by a subcontract with Matrix Research, Inc. for research sponsored by the Air Force Research Laboratory under contract FA8650-14-D-1722.

The Wigner-Ville distribution (WVD) is often regarded as the prototype bi-linear TF representation (TFR) and is known to provide the best resolution for mono-component linear FM signals [3]. However, it generates excessive cross-terms in the case of multi-component or non-linear FM signals. TFR reconstruction in the presence of missing samples has been considered in several studies by exploiting TF kernels and compressive sensing-based techniques [4]–[11]. Generally, data-dependent TF kernels, such as the adaptive optimal kernel (AOK) [12] and the adaptive directional TF distribution (ADTFD) [13], are found more effective in cross-term suppression and artifact mitigation. The recently developed missing data iterative sparse reconstruction (MI-SR) approach [4] provides reliable TFR recovery by combining the cross-term suppression capabilities of the signal-adaptive TF kernels and the missing data recovery obtained by iteratively utilizing the orthogonal matching pursuit (OMP) [14].

However, in the case of multi-component non-linear FM signals with distinct amplitude levels and in the presence of burst missing data samples, the aforementioned approaches may fail to estimate the IF signatures for the weak signals. Recently, the adaptive local filtering-based directional time-frequency distribution (ALF-DTFD) [15] was introduced to provide high-resolution IF estimation for both strong and weak signals by adapting the threshold, based on the local maximum values of the signal captured within a window of a specified length at each time instant. However, the success of the ALF-DTFD heavily depends on the quality of the underlying TFR, which is the major drawback of this approach. On the other hand, the generalized stepwise demodulation transform technique [16], developed based on the synchro-squeezing transform, sequentially estimates each signal component using the demodulation operation. However, it requires an accurate estimation of the phase law of each signal component as a demodulating operator, which is often difficult to obtain in the case of multi-component non-linear FM signals.

Various techniques based on signal subtraction, subspace projection, and signal stationarization have been proposed for non-stationary FM interference suppression in communication signals [17]–[20]. Because methods based on direct signal subtraction are sensitive to the accuracy of the estimated phases, subspace projection-based techniques are often used, provided that the signal IF is accurately estimated. In the presence of missing samples, a similar approach that stationarizes (demodulate) the strong FM signal into a direct current (DC) component based on the estimated IF. This procedure was introduced in [20] to successfully remove a single FM jammer in anti-jamming GPS receiver.

In this paper, we extend this method to consider the challenging problem of accurate IF estimation of multi-component non-linear FM signals with distinct signal strengths and in the presence of burst missing data samples. Compared with the work presented in [20] which mainly focused on the excision of a single strong FM signal, the problem considered in this study is more challenging because we consider multiple FM signal components, and some of them are weak. Note that directly applying the sparse reconstruction methods, such as the orthogonal matching pursuit (OMP), would fail in the underlying scenario to provide accurate IF estimation for the weak signal components [15].

To solve this issue, we propose a sequential estimation-based approach, referred to as Sequential Missing data Estimation-based Time-Frequency Representation (SME-TFR). First, we obtain the TFR of the received signal with burst missing samples. While a number of methods can be used to obtain the required TFR, we consider signal-adaptive TF kernel-based approaches, and the AOK is used as an example to demonstrate its capability of effectively mitigating cross-terms and artifacts. The obtained IF of the strongest signal component is estimated using a peak detection technique. We then construct the time-domain signal waveform using the estimated IFs, which is used to remove the strongest component from the received signal through orthogonal projection. The weaker signals are successively detected and suppressed. As the refined estimation of the weaker components is independent of the missing data positions, the effects of the artifacts due to the burst missing samples are suppressed in the resulting TFRs, and energy concentration of the TFRs is preserved.

Notations. A lower (upper) case bold letter denotes a vector (matrix). $(\cdot)^{\mathrm{T}}$, and $(\cdot)^{\mathrm{H}}$, respectively, represent transpose and Hermitian. $\mathcal{F}_x(\cdot)$ defines the discrete Fourier transform (DFT) with respect to x. Notation $\underset{t}{*}$ indicates convolution with respect to t.

II. Signal Model and Reduced-Interference Distributions

A. Signal Model

Consider a discrete-time multi-component analytic FM signal, expressed as

$$s[t] = \sum_{k=1}^{K} s_k[t], \qquad t = 1, ..., T, \tag{1}$$

where

$$s_k[t] = a_k \exp(j\phi_k[t]), \qquad t = 1, ..., T, \tag{2}$$

is the kth signal component, $k = 1, ..., K$. In the above expression, a_k and $\phi_k[t]$ are, respectively, the amplitude and time-varying phase of the kth signal component. We label the signal components according to their amplitude levels, from the highest to the lowest, i.e., $a_1 \geq a_2 \geq ... \geq a_K$. Assume that there are B mutually non-overlapping missing data bursts, and denote N_b as the number of missing samples in the bth burst, $b = 1, ..., B$. The positions of the missing data bursts are assumed to be randomly distributed over time. The total number of the burst missing data samples is $N = \sum_{b=1}^{B} N_b,\ 0 \leq N < T$.

Let $\mathcal{S} \subset \{1, ..., T\}$ be the set of observed time instants with a cardinality of $|\mathcal{S}| = T - N$. As such, the observed signal, $r[t]$, can be expressed as the product of $s[t]$ and an observation mask, $R[t]$, i.e.,

$$r[t] = s[t] \cdot R[t], \tag{3}$$

where

$$R[t] = \begin{cases} 1, & \text{if } t \in \mathcal{S}, \\ 0, & \text{if } t \notin \mathcal{S}. \end{cases} \tag{4}$$

B. Reduced-Interference Distributions

The utilization of TF kernels renders effective reduced-interference TF distributions to effectively suppress undesired effects of cross-terms and artifacts due to the missing samples. The kernel operation in the IAF domain can be represented as a mixed multiplication/convolution operation. Denote $C_{ss}[t, \tau]$ as the IAF of $s[t]$, which is defined in the time-lag (t-τ) domain as

$$C_{ss}[t, \tau] = s\left[t + \tau\right] s^*\left[t - \tau\right]. \tag{5}$$

Then, a general form of the reduced-interference TF distribution, $D_{\mathrm{RID}}[t, f]$, is given by

$$\begin{aligned} D_{\mathrm{RID}}[t, f] &= \mathcal{F}_\tau\left[\Phi[t, \tau] \underset{t}{*} C_{ss}[t, \tau]\right], \\ &= \mathcal{F}_\tau\Big[\sum_u \Phi[t-u, \tau] C_{ss}[u, \tau]\Big], \\ &= \sum_\tau \sum_u \Phi[t-u, \tau] C_{ss}[u, \tau] e^{-j4\pi f \tau}, \end{aligned} \tag{6}$$

where $\Phi[t, \tau]$ is the TF kernel function. Note that, in (6), 4π is used instead of 2π, because the lag in (5) is 2τ.

III. Proposed Sequential Estimation Technique

Multi-component non-linear FM signals exhibit severe cross-terms between components. Additionally, burst missing samples introduce sinc-like artifact patterns in the TFR of these signals, which are concentrated around the true IFs of the signal components. Such cross-terms and the artifacts, particularly those due to the strong signal components, make the identification of signal IFs, notably those of the weaker signal components, challenging. In this section, we describe the proposed Sequential Missing data Estimation-based Time-Frequency Representation (SME-TFR) approach, with the aim to provide an accurate IF and magnitude estimation of all signal components, while mitigating the undesired effects of cross-terms and artifacts from the underlying TFRs.

Without loss of generality, we refer to the strongest signal component as the first component, and the weakest signal component is referred to as the last component. The signal components are iteratively reconstructed in the order, from the first component to the last component, as follows:

(i) The iteration counter, i, is initialized as 1. Denote the received multi-component FM signal as the initial residual signal, $\mathbf{r}^{(0)} = \mathbf{r} = [r_1, ..., r_T]^{\mathrm{T}}$.

(ii) Compute the reduced-interference TFR, $\bar{D}_{\mathrm{RID}}^{(i-1)}[t,f]$ from $\mathbf{r}^{(i-1)}$ using (5) and (6). The AOK is used as the kernel in this paper. From $\bar{D}_{\mathrm{RID}}^{(i-1)}[t,f]$, we obtain the estimated IF vector of the ith signal component, $\hat{\mathbf{f}}_i = [\hat{f}_{i1}, ..., \hat{f}_{iT}]^{\mathrm{T}}$, through peak detection in the TFR. That is, at each time instant t, the frequency that corresponds to the maximum valued peak along the frequency axis is identified as the IF estimate $\hat{f}_{it}$ of the ith signal component at that time. The collection of all $(t, \hat{f}_{it})$ pairs forms the sparse TFR basis $\bar{S}_{\mathrm{RID}}^{(i)}[t,f]$ of the ith signal component.

(iii) Using estimated IFs, the phase information at each time instant is obtained as $\phi_i(t) = 2\pi \sum_t \hat{f}_{it}$. Based on this result, we estimate the signal basis as $\hat{\mathbf{s}}_i = [\hat{s}_{i1}, ..., \hat{s}_{iT}]^{\mathrm{T}}$ with $\hat{s}_{it} = \exp(j\phi_i[t])$. The complex amplitude of the ith component is estimated through the following projection:

$$\begin{aligned}\hat{\alpha}_i &= \frac{1}{T-N}\hat{\mathbf{s}}_i^{\mathrm{H}}\mathbf{r}^{(i-1)}, \\ &= \frac{1}{T-N}\sum_{t\in\mathcal{S}}\left(a_i[t] + \sum_{q=i+1}^{K} a_q[t]e^{j(\phi_q[t]-\phi_i[t])}\right), \\ &\approx \frac{1}{T-N}\sum_{t\in\mathcal{S}} a_i[t],\end{aligned} \tag{7}$$

which yields the average of $a_i[t]$. As such, the estimated ith component becomes $\hat{\mathbf{r}}_i = \hat{\alpha}_i\hat{\mathbf{s}}_i = [\hat{r}_{i1}, ..., \hat{r}_{iT}]^{\mathrm{T}}$.

(iv) The signal component $\hat{\mathbf{r}}_i$ is subtracted from $\mathbf{r}^{(i-1)}$ to obtain the residual signal

$$\mathbf{r}^{(i)} = \mathbf{r}^{(i-1)} - \hat{\mathbf{r}}_i = \mathbf{r}^{(i-1)} - \hat{\alpha}_i\hat{\mathbf{s}}_i. \tag{8}$$

(v) The iteration counter is increased by 1 and the steps (ii)–(iv) are repeated until the residual becomes negligible. Thus, all the signal components are successively estimated and compensated for. The final value of i provides the total number of components K.

(vi) The refined estimated signal is obtained as $\hat{\mathbf{s}} = \sum_{i=1}^{K}\hat{\mathbf{r}}_i = \sum_{i=1}^{K}\hat{\alpha}_i\hat{\mathbf{s}}_i$, and the corresponding robust reduced-interference TFR is achieved as $\bar{S}_{\mathrm{RID}}[t,f] = \sum_{i=1}^{K}|\hat{\alpha}_i|^2\bar{S}_{\mathrm{RID}}^{(i)}[t,f]$. The final estimated signal, $\hat{\mathbf{s}}$, and the corresponding, $\bar{S}_{\mathrm{RID}}[t,f]$, have achieved effective suppression of the cross-terms and artifacts.

IV. Simulation Results

To clearly demonstrate the effectiveness of the proposed SME-TFR approach, we consider a two-component FM signal with different amplitudes, given by

$$y(t) = \exp(j\phi_1(t)) + 0.4\exp(j\phi_2(t)), \quad t = 1, ..., T, \tag{9}$$

where T is chosen to be 128 and the instantaneous phase laws of these two components are respectively expressed as,

$$\begin{aligned}\phi_1(t) &= 2\pi(0.05t + 0.001t^2/T + 0.10t^3/T^2), \\ \phi_2(t) &= 2\pi(0.15t + 0.003t^2/T + 0.08t^3/T^2).\end{aligned} \tag{10}$$

In order to clearly understand the effects of the burst missing samples on the reconstruction performance, we consider the noise-free case.

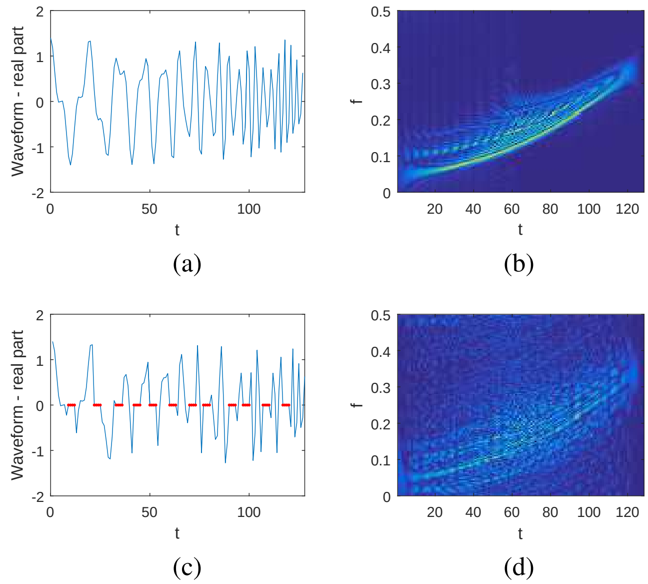

Fig. 1 Signal waveform and WVD: (a) Real part of the original signal; (b) WVD of the original signal; (c) Real part of the received signal with burst missing samples; (d) WVD of the received signal.

Figs. 1(a) and 1(b) respectively show the real part of the original signal waveform without missing samples and the corresponding WVD. Due to the bilinear nature of the underlying multi-component FM signal, the WVD exhibits excessive cross-terms. The real part of the received signal waveform, which contains a total of 48 (i.e., 37.5%) burst missing samples, and the corresponding WVD are respectively depicted in Figs. 1(c) and 1(d). The missing data positions are marked with red dots. These missing samples are clustered into $B = 12$ bursts, with each burst containing 4 missing samples. The burst missing samples generate convolutive sinc-function-like artifact patterns in the resulting TFR, as clearly shown in Fig. 1(d). Note that, unlike the random missing data case, where the artifacts are uniformly distributed in the entire TF region [5], the artifacts due to the burst missing samples are concentrated around true IFs [4]. This fact makes spectral estimation and analysis much more challenging. The effects of these artifacts are difficult to be mitigated with a TF kernel alone.

Fig. 2(a) displays the TFR of the original received signal with burst missing samples. As seen in the TFR of Fig. 2(a), the cross-terms, artifacts, and aliasing signatures around the weaker signal component, make the detection of the weak signal component challenging. Figs. 2(c) and 2(d) respectively present the estimated TFRs of the first and the second signal components, whereas Fig. 2(b) shows the combined TFR of both signal components. As seen in these Figures, the undesired effects of cross-terms and artifacts are mitigated, the energy concentration of the TFRs is improved, and an accurate estimation of the signal components is achieved. In all the above TFRs, the AOK is applied for fine TFR estimation, and the value of the kernel volume is chosen as 2.

Figs. 2(e) and 2(f), respectively, provide the estimated IFs of the two signals, overlaid with their respective true IFs. The IFs of both signal components are precisely estimated with an

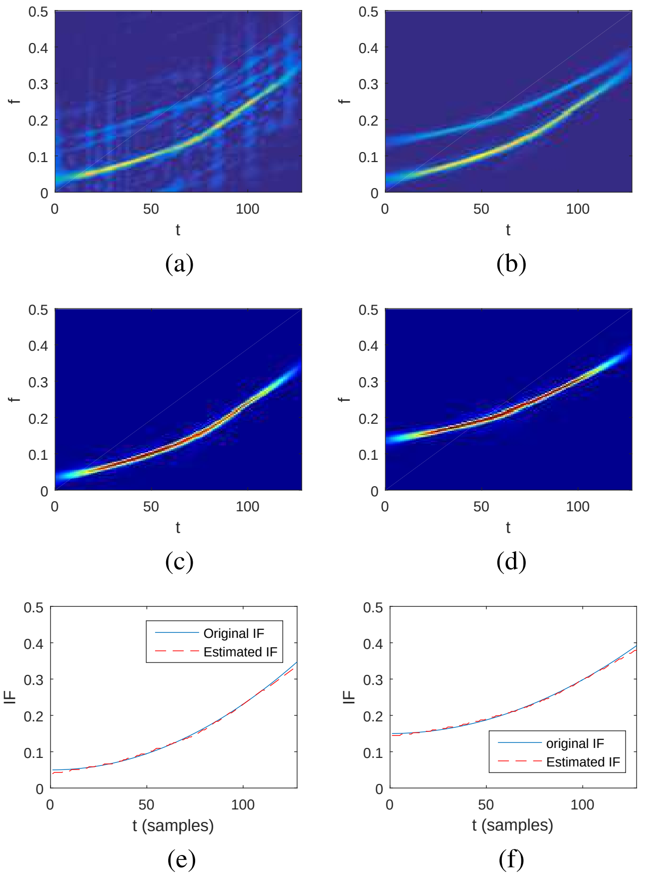

Fig. 2 Estimated results: (a) TFR of the original received signal; (b) TFR of the refined estimated signal; (c) TFR of the estimated stronger component; (d) TFR of the estimated weaker component; (g) Estimated IF of the stronger component; (h) Estimated IF of the weaker component.

average error of 0.0035 and 0.0039, respectively, measured in terms of the normalized frequency. Note that the information regarding the amplitude level is also preserved. The average amplitudes obtained for the two signal components are 1.0000 and 0.4025, respectively, which are very close to the actual amplitudes of 1.0000 and 0.4000.

Figs. 3(a) and 3(b), respectively, show the estimated real-part waveform and phase of the first (stronger) signal component, overlaid with those of the original signal, and Fig. 3(c) shows the unwrapped phase estimation error. All the phase values are shown in radians. As seen in Fig. 3, this signal component is estimated accurately, except for the deviation at few places.

Similarly, the comparison of the estimated real-part waveform and phase of the second (weaker) signal component, with respect to their original signal counterparts, are respectively provided in Figs. 4(a) and 4(b). As seen in these plots, the weaker signal component is accurately estimated except for the deviation at a few places. The unwrapped phase estimation error is displayed in Fig. 4(c). The estimation accuracy of the weaker signal component is sensitive to the IF estimation and the frequency quantization errors of the stronger signal component. Therefore, in Fig. 4(c), the overall error in the estimated phase is slightly higher for the weaker signal component than

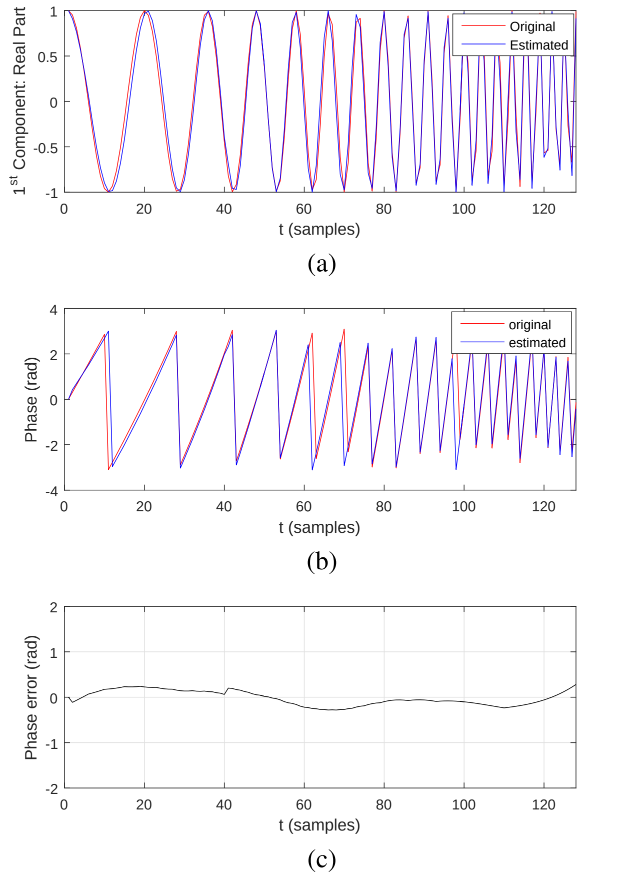

Fig. 3 Reconstructed results of the stronger signal component: (a) Real-part waveform; (b) Phase; (c) Unwrapped phase estimation error.

that of the stronger signal component shown in Fig. 3(c).

V. Conclusions

In this paper, we present a new technique to accurately reconstruct non-linear, multi-component FM signals with distinct amplitude levels, in the presence of burst missing data samples. While conventional approaches fail to recover weak signal components in such scenarios due to the undesired effects of the cross-terms and artifacts, the proposed SME-TFR approach successfully resolves all signal components with high IF accuracy through effective mitigation of cross-terms and artifacts, while maintaining the energy concentration of desired signal components. The effectiveness of the proposed method is examined through experimental results.

References

[1] A. Papandreou-Suppappola (Ed.), *Applications in Time-Frequency Signal Processing*, CRC Press, 2002.

[2] B. Boashash (Ed.), *Time-Frequency Signal Analysis and Processing, 2nd Ed.* Academic Press, 2016.

[3] L. Cohen, "Time-frequency distributions – A review," *Proc. IEEE*, vol. 77, no. 7, pp. 941–981, July 1989.

[4] V. S. Amin, Y. D. Zhang, and B. Himed, "Sparsity-based time-frequency representation of FM signals with burst missing samples," *Signal Process.*, vol. 155, pp. 25–43, Feb. 2019.

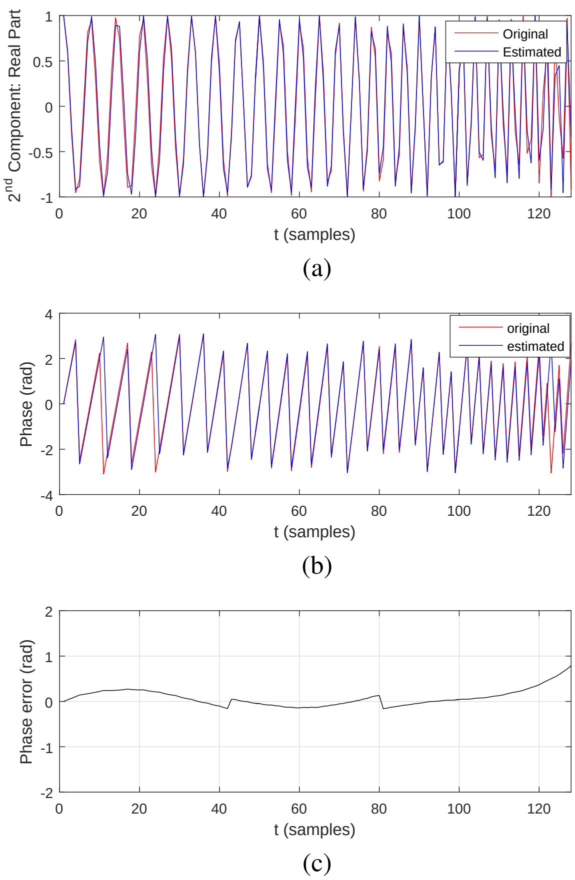

Fig. 4 Reconstructed results of the weaker signal component: (a) Real-part waveform; (b) Phase; (c) Unwrapped phase estimation error.

[5] Y. D. Zhang, M. G. Amin, and B. Himed, "Reduced interference time-frequency representations and sparse reconstruction of undersampled data," in *Proc. European Signal Process. Conf.*, Marrakech, Morocco, Sept. 2013, pp. 1–5.

[6] Q. Wu, Y. D. Zhang, and M. G. Amin, "Continuous structure based Bayesian compressive sensing for sparse reconstruction of time-frequency distributions," in *Proc. Int. Conf. Digital Signal Process.*, Hong Kong, China, Aug. 2014, pp. 831–836.

[7] L. Stankovic, S. Stankovic, I. Orovic, and Y. D. Zhang, "Time-frequency analysis of micro-Doppler signals based on compressive sensing," in M. Amin (Ed.), *Compressive Sensing for Urban Radars*, CRC Press, 2014.

[8] B. Jokanovic, M. G. Amin, Y. D. Zhang, and F. Ahmad, "Multi-window time-frequency signature reconstruction from undersampled continuous wave radar measurements for fall detection," *IET Radar Sonar Nav.*, vol. 9, no. 2, pp. 173–183, Feb. 2015.

[9] M. G. Amin, B. Jokanovic, Y. D. Zhang, and F. Ahmad, "A sparsity-perspective to quadratic time-frequency distributions," *Digital Signal Process.*, vol. 46, pp. 175–190, Nov. 2015.

[10] Y. D. Zhang, "Resilient quadratic time-frequency distribution for FM signals with gapped missing data," in *Proc. IEEE Radar Conf.*, Seattle, WA, May 2017, pp. 1765–1769.

[11] S. Zhang and Y. D. Zhang, "Robust time-frequency analysis of multiple FM signals with burst missing samples," *IEEE Signal Process. Lett.*, vol. 26, no. 8, pp. 1172–1176, June 2019.

[12] D. L. Jones and R. G. Baraniuk, "An adaptive optimal-kernel time-frequency representation," *IEEE Trans. Signal Process.*, vol. 43, no. 10, pp. 2361–2371, Oct. 1995.

[13] N. Khan and B. Boashash, "Multi-component instantaneous frequency estimation using locally adaptive directional time frequency distributions," *Int. J. Adaptive Control Signal Process.*, vol. 30, pp. 429–442, March 2016.

[14] J. A. Tropp and A. C. Gilbert, "Signal recovery from random measurements via orthogonal matching pursuit," *IEEE Trans. Inf. Theory*, vol. 53, no. 12, pp. 4655–4666, Dec. 2007.

[15] V. S. Amin, Y. D. Zhang, and B. Himed, "Improved Instantaneous Frequency Estimation of Multi-component FM signals," in *Proc. IEEE Radar Conf.*, Boston, MA, April 2019.

[16] J. Shi, M. Liang, D.-S. Necsulescu, and Y. Guan, "Generalized stepwise demodulation transform and synchrosqueezing for time–frequency analysis and bearing fault diagnosis," *J. Sound Vibr.*, vol. 368, pp. 202–222, April 2016.

[17] M. G. Amin and A. N. Akansu, "Time-frequency for interference excision in spread spectrum communications," in "Highlights of signal processing for communications: Celebrating a half century of signal processing," *IEEE Signal Process. Mag.*, vol. 16, no. 2, March 1999.

[18] S. Barbarossa and A. Scaglione, "Adaptive time-varying cancellation of wideband interferences in spread-spectrum communications based on time–frequency distributions," *IEEE Trans. Signal Process.*, vol. 47, no. 4, pp. 957–965, April 1999.

[19] Y. Zhang and M. G. Amin, "Array processing for nonstationary interference suppression in DS/SS communications using subspace projection techniques," *IEEE Trans. Signal Process.*, vol. 49, no. 12, pp. 3005–3014, Dec. 2001.

[20] M. G. Amin and Y. D. Zhang, "Nonstationary jammer excision for GPS receivers using sparse reconstruction techniques," in *Proc. ION GNSS+*, Tampa, FL, Sept. 2014, pp. 3469–3474.

[21] Y. D. Zhang, M. G. Amin, and B. Himed, "Direction-of-arrival estimation of nonstationary signals exploiting signal characteristics," in *Proc. Int. Conf. Info. Sci. Signal Process. Appl.*, Montreal, Canada, July 2012, pp. 1223–1228.